` 3,5-bisphosphate production has pleiotropic effects on various membrane trafficking routes in Arabidopsis

Hirano, T.; Munnik, T.; Sato, M.H.

DOI
10.1093/pcp/pcw164

Publication date
2017

Document Version
Final published version

Published in
Plant and Cell Physiology

PCP
PLANT & CELL PHYSIOLOGY

Regular Paper

Inhibition of phosphatidylinositol 3,5-bisphosphate production has pleiotropic effects on various membrane trafficking routes in Arabidopsis

Tomoko Hirano[1,*], Teun Munnik[2] and Masa H. Sato[1,*]

[1]Laboratory of Cellular Dynamics, Graduate School of Life and Environmental Sciences, Kyoto Prefectural University, Kyoto, 606-8522 Japan
[2]Plant Physiology, Swammerdam Institute for Life Sciences, University of Amsterdam, Amsterdam, The Netherlands
*Corresponding authors: Tomoko Hirano, E-mail, thirano@mei.kpu.ac.jp; Fax, +81-75-703-5448; Masa H. Sato, E-mail, mhsato@kpu.ac.jp; Fax, +81-75-703-5448.
(Received May 4, 2016; Accepted September 15, 2016)

Phosphoinositides play an important role in various membrane trafficking events in eukaryotes. One of them, however, phosphatidylinositol 3,5-bisphosphate [PI(3,5)P_2], has not been studied widely in plants. Using a combination of fluorescent reporter proteins and the PI(3,5)P_2-specific inhibitor YM202636, here we demonstrated that in *Arabidopsis thaliana*, PI(3,5)P_2 affects various membrane trafficking events, mostly in the post-Golgi routes. We found that YM201636 treatment effectively reduced PI(3,5)P_2 concentration not only in the wild type but also in *FAB1A*-overexpressing Arabidopsis plants. In particular, reduced PI(3,5)P_2 levels caused abnormal membrane dynamics of plasma membrane proteins, AUX1 and BOR1, with different trafficking patterns. Secretion and morphological characteristics of late endosomes and vacuoles were also affected by the decreased PI(3,5)P_2 production. These pleiotropic defects in the post-Golgi trafficking events were caused by the inhibition of PI(3,5)P_2 production. This effect is probably mediated by the inhibition of maturation of FAB1-positive late endosomes, thereby impairing late endosome function. In conclusion, our results imply that in Arabidopsis, late endosomes are involved in multiple post-Golgi membrane trafficking routes including not only vacuolar trafficking and endocytosis but also secretion.

Keywords: *Arabidopsis thaliana* • FAB1/PIKfyve • Phosphatidylinositol 3,5-bisphosphate • Post-Golgi membrane trafficking routes • YM201636.

Abbreviations: AUX1, auxin 1; BOR1, high boron 1; DMSO, dimethylsulfoxide; ER, endoplasmic reticulum; FAB1, formation of haploid and binucleate cells 1; FYVE, FAB1 YPTB VAC1 EEA1; GFP, green fluorescent protein; mRFP, monomeric red fluorescent protein; MS, Murashige and Skoog; PIKfyve, a FYVE finger-containing phosphoinositide kinase; PI3P, phosphatidylinositol 3-phosphate; PI(3,5)P_2, phosphatidylinositol 3,5-bisphosphate; TGN, *trans*-Golgi network; TLC, thin-layer chromatography; VAMP727, **v**esicle-associated membrane protein 727; WT, wild type; YFP, yellow fluorescent protein. Sequence data from this article can be found in the Arabidopsis Information Resource (http://www.arabidopsis.org/) under the following accession numbers: *AUX1* (At2g38120), *AtVAM3/SYP22* (At5g46860), *BOR1* (At2g47160), *FYVE1* (At1g20110), *FAB1B* (At3g14270), *FAB1A* (At4g33240) and *UBQ10* (At4g05320).

Introduction

Membrane trafficking in eukaryotes represents the process of transport of proteins and lipids from the endoplasmic reticulum (ER) to various membrane organelles including the Golgi apparatus, *trans*-Golgi network (TGN), endosomes, vacuoles or the plasma membrane, or the transport of secretory vesicles to the extracellular space via vesicular traffic underlying various biological processes. In this process, newly synthesized proteins in the ER are passing through the Golgi apparatus, then cargo proteins are sorted into the vacuolar sorting or secretory pathways in the TGN (Jahn et al. 2003, Bonifacino and Glick 2004). In mammalian cells, the TGN is usually localized to the *trans*-most side of the Golgi apparatus; however, in plants, the TGN not only overlaps the Golgi apparatus but also exists in the form of independent organelles dispersed throughout the cytoplasm (Uemura et al. 2004, Kang et al. 2011). In the plant secretory pathway, TGN-derived secretory vesicles form clustered structures, termed secretory vesicle clusters (Toyooka et al. 2009) or secretory vesicles released from the TGN (Staehelin and Chapman, 1987 Winter et al. 2007). Secretory vesicle clusters or secretory vesicles move directly to and fuse with the plasma membrane in various dividing and growing plant cells. In the vacuolar sorting pathway, cargo proteins use at least three distinct routes: (i) the RAB5/RAB7-dependent route via late endosomes; (ii) the multivesicular body/AP-3-dependent route; and (iii) the RAB5-dependent AP-3-independent route (Ebine et al. 2014). Morphologically and immunocytochemically, secretory vesicle clusters and secretory vesicles are clearly distinct from multivesicular bodies, suggesting that the plant secretory pathway never passes through multivesicular bodies to the plasma membrane (Kang et al. 2011). Nonetheless, unique to plants, late-endosomal RAB5, Arabidopsis RAB5

Plant Cell Physiol. 58(1): 120–129 (2017) doi:10.1093/pcp/pcw164, Advance Access publication on 1 November 2016, available online at www.pcp.oxfordjournals.org

(ARA6) and vesicle-associated membrane protein (VAMP)/R-soluble *N*-ethylmaleimide sensitive factor (NSF) attachment protein receptor (SNARE), VAMP727, are reported to be involved in both vacuolar and secretion pathways, pointing to the existence of an alternative pathway to the plasma membrane, via late endosomes or multivesicular bodies in the salinity stress response (Ebine et al. 2011).

In contrast to mammalian TGNs, plant TGNs also function as early endosomes, into which endocytic proteins are delivered for recycling or degradation (Dettmer et al. 2006). Endocytic sorting of plasma membrane proteins from the plasma membrane into the TGN/early endosomes is followed either by recycling to particular domains in the plasma membrane or by further sorting into late endosomes/multivesicular bodies for their ultimate degradation in the lytic vacuole (Park and Jürgens 2011, Drakakaki and Dandekar 2013).

Taken together, these data suggest that the post-Golgi trafficking pathways, including exocytosis, secretion, the vacuole, endocytosis and recycling pathways, are passing though the TGN/early endosomes. In plants, the involvement of late endosomes/multivesicular bodies in the post-Golgi trafficking pathways is poorly understood.

Phosphoinositides play important roles in various membrane trafficking events (Balla 2013). For example, phosphatidylinositol 3-phosphate (PI3P), phosphatidylinositol 4-phosphate (PI4P), phosphatidylinositol 3,5-bisphosphate [$PI(3,5)P_2$] and phosphatidylinositol 4,5-bisphosphate [$PI(4,5)P_2$] perform essential functions in endosomal trafficking, secretion and vacuolar sorting (Krishnamoorthy et al. 2014, Heilmann and Heilmann 2015). PI3P is produced from phosphatidylinositol by class III PI3-kinase, vacuolar protein sorting 34 (VPS34). In animal cells, PI3P is predominantly localized to the early endosomes and controls endosome maturation, recycling and degradation of cargo proteins in co-ordination with Rab5 GTPases (Jean and Kiger 2012). In contrast, in Arabidopsis, PI3P mainly resides in late endosomes and prevacuolar membranes (Vermeer et al. 2006, Simon et al. 2014); this observation is indicative of the dual function of late endosomes/multivesicular bodies in plants.

$PI(3,5)P_2$ is produced from PI3P by the enzymatic action of phosphatidylinositol 3-phosphate 5-kinase termed formation of haploid and binucleate cells 1 (FAB1), which in animal cells is called FYVE finger-containing phosphoinositide kinase (PIKfyve); in both cases, this protein drives late-endosome maturation (Jean and Kiger 2012, McCartney et al. 2014). The Arabidopsis genome codes for four FAB1 genes (FAB1A–FAB1D), of which only FAB1A and FAB1B contain a FYVE domain. The Arabidopsis *fab1a/fab1b* double mutant shows male gametophyte mortality. Mutant pollen grains show severe defects in vacuolar reorganization after the first mitotic division during development; these data are suggestive of the importance of FAB1 and $PI(3,5)P_2$ in vacuolar rearrangement for pollen development (Whitley et al. 2009). Conditional down-regulation of *FAB1A* and *FAB1B* expression causes various abnormal phenotypes, including retarded growth, hypersensitivity to an exogenous auxin, disturbance of root gravitropism, and a few floral organ abnormalities because of several endomembrane homeostasis impairments affecting endocytosis, vacuole formation and vacuolar acidification (Hirano et al. 2011). In addition, we recently found that FAB1 is essential for the process of maturation of late endosomes (from TGN/early endosomes) intended to establish an association between cortical microtubules and late endosomes (Hirano et al. 2015).

It was reported that YM201636 is a selective inhibitor of PIKfyve, blocking $PI(3,5)P_2$ production and regulating a number of intracellular membrane trafficking pathways without disturbing other PIP kinases and protein kinase B functions in mammals (Jefferies et al. 2008). In Arabidopsis, YM201636 treatment reduces vacuolar acidification and convolution of guard cells, and delays the stomatal closure in response to ABA (Bak et al. 2013). We showed previously that YM201636 specifically reduces $PI(3,5)P_2$ production without affecting the concentration of any other phosphoinositides, and can accurately mimic *FAB1A/B* conditional mutant phenotypes in Arabidopsis (Hirano et al. 2015).

Here, we studied how $PI(3,5)P_2$ affects various transport pathways using a combination of the FAB1-specific inhibitor YM201636 and various fluorescent protein markers for the post-Golgi membrane trafficking in *Arabidopsis thaliana*. We found that the $PI(3,5)P_2$ concentration that is reduced by YM201636 treatment impairs borate-dependent endocytosis and degradation of a plasma membrane protein, BOR1 (high boron 1), as well as the uptake of an exogenous auxin, secretion of a fluorescent secretory marker protein and morphological characteristics of late endosomes and the central vacuole. These results suggest that in plants, most post-Golgi membrane trafficking routes converge on FAB1-positive late endosomes.

Results

Balanced $PI(3,5)P_2$ levels are crucial for Arabidopsis growth

We previously reported that a FAB1/PIKfyve inhibitor, YM201636, specifically inhibits $PI(3,5)P_2$ production in wild-type (WT) Arabidopsis seedlings (Hirano et al. 2015). Here, we first evaluated the inhibitory effect of YM201636 in two *FAB1A*-overexpressing *A. thaliana* lines. As reported previously, the *FAB1A*-overexpressing lines #10 and #34 overexpress *FAB1A* at different magnitudes and show accompanying growth inhibition (Hirano et al. 2011). Measurement of $PI(3,5)P_2$ levels in these two lines by ^{32}P-labeling and thin-layer chromatography (TLC) revealed that the concentration of $PI(3,5)P_2$ was significantly increased in the two *FAB1A*-overexpressing lines compared with WT Arabidopsis [37.8% overexpression in line #10 and 107% overexpression in line #34 compared with the WT dimethylsulfoxide (DMSO) control], without affecting the level of other phospholipids (**Supplementary Fig. S1**). YM201636 (1 μM) decreased $PI(3,5)P_2$ levels by 50–80% (by 66.9% in the WT, by 76.1% in line #10 and by 81.1% in line #34; **Fig. 1A**). The growth inhibition of root length of the *FAB1A*-overexpressing line #34 was suppressed by treatment with YM201636 in a dose-dependent manner (**Fig. 1B**). Because we previously

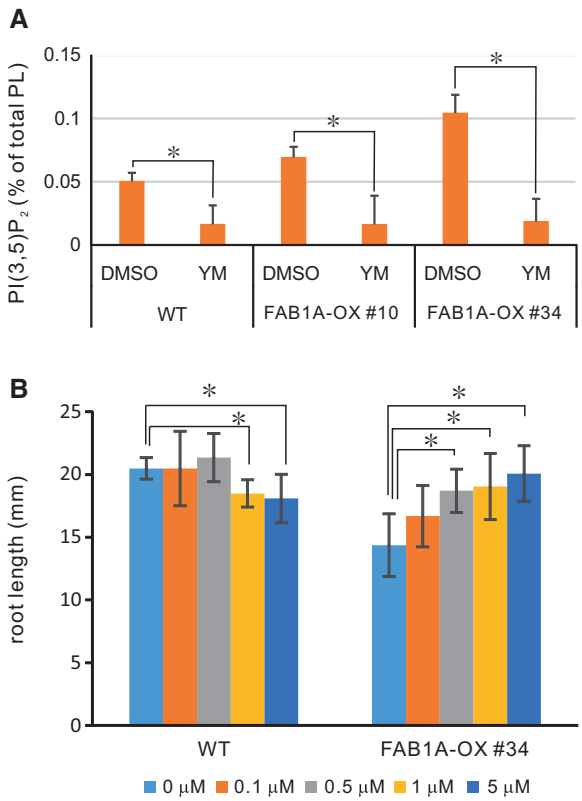

Fig. 1 YM201636 inhibits PI(3,5)P_2 production in an *FAB1A*-overexpressing line and causes a root growth defect. (A) Five-day-old seedlings were labeled overnight with $^{32}P_i$, and incubated for an additional 2 h in the presence (+YM) or absence (DMSO) of 1 μM YM201636. Total phospholipids were then extracted, separated by TLC, and quantified by phosphoimaging. Data are expressed as percentages of total [^{32}P]phospholipids and are presented as mean ± SD of three independent samples containing three seedlings each. Significant differences between seedlings incubated with or without YM201636 are indicated by an asterisk (Student's *t*-test, $P < 0.001$). (B) WT and the *FAB1A*-overexpressing line (FAB1A-OX #34) were grown on 1/2 MS medium with 0, 0.1, 0.5, 1.0 and 5.0 μM YM201636 for 8 d, then the root length of these seedlings was measured. Significant differences between control and YM201636-treated seedlings are indicated by an asterisk (Student's *t*-test, $P < 0.001$; $n > 9$). Experiments were repeated three times, and yielded similar results.

showed that the loss and gain of FAB1 function cause the same growth defect in Arabidopsis (Hirano et al. 2011), the present data indicate that balanced PI(3,5)P_2 levels are crucial for proper Arabidopsis growth.

Exogenous auxin uptake is reduced by YM201636 treatment

Previously, we reported that exogenous non-penetrating auxin-induced lateral root formation is inhibited by the reduction in *FAB1A/B* expression, suggesting that the influx carrier-dependent auxin uptake is impaired by inhibition of PI(3,5)P_2 synthesis (Hirano et al. 2011). Therefore, we next tested whether exogenous non-penetrating auxin uptake is also affected by YM201636. To visualize auxin uptake, Arabidopsis seedlings with the *DR5rev:GFP* auxin reporter line were treated with 1 μM non-penetrating auxin, i.e. IAA, in the presence of 1 μM YM201636. In the absence of exogenous IAA, the intensity of green fluorescent protein (GFP) fluorescence in the root tip region was unchanged in the presence or absence of YM201636 (**Fig. 2A, B**). In contrast, strong GFP fluorescence was detected in whole-root tissues grown on a medium containing IAA (**Fig. 2C**) although GFP fluorescence was significantly decreased when the seedlings were grown on a medium containing 1 μM YM201636, even though 1 μM IAA was exogenously administered (**Fig. 2D**). Conditional knockdown of FAB1A/B genes gave similar results (**Supplementary Fig. S2**). These findings suggest that uptake of exogenous auxins is severely impaired by inhibition of PI(3,5)P_2 synthesis.

We hypothesized that the PI(3,5)P_2-dependent changes in auxin uptake might be caused by a change in the plasma membrane localization of the auxin influx carrier protein, auxin 1 (AUX1). To test this hypothesis, we analyzed the localization of the AUX1–yellow fluorescent protein (YFP) fusion protein in the root tip region in the presence and absence of YM201636. As shown in **Fig. 2E and F**, 5 h treatment with YM201636 dramatically decreased the intensity of AUX1–YFP fluorescence on the plasma membrane. To determine whether this decrease in AUX1–YFP fluorescence was due to proteasomal degradation or to endocytic retrieval from the plasma membrane, we treated the cells with a proteasome inhibitor, MG132 (6 h, 50 μM) or a V-ATPase inhibitor, concanamycin A (1 h, 2 μM). The YM201636-dependent decrease in AUX1–YFP fluorescence was not affected by MG132 treatment (**Fig. 2G, R**) but was abrogated by concanamycin A (**Fig. 2H, R**). We observed the same results in *FAB1A/B*-artificial microRNA (amiRNA) plants (**Supplementary Fig. S3**). In the presence of YM201636, AUX1–YFP was internalized and formed punctate structures beneath the plasma membrane after 2.5 h incubation (**Fig. 2L–N**), then the structures disappeared after 5 h incubation (**Fig. 2O–Q**). Next, we measured the *AUX1* mRNA expression level in 5-day-old WT seedlings after YM201636 treatment and found that *AUX1* mRNA expression did not change after YM201636 treatment (**Fig. 2S**), suggesting that the YM201636-dependent inhibition of AUX1–YFP fluorescence does not take place at the transcriptional level. Because concanamycin A is known to block the endocytic transport pathway to the tonoplast from the TGN (Dettmer et al. 2006), the YM201636-dependent sequestration of AUX1–YFP is likely to be blocked in the TGN. Taken together, these results indicated that YM201636-induced down-regulation of AUX1 might be mediated by endocytosis and is followed by degradation in the vacuole.

PI(3,5)P_2 regulates degradation and expression of BOR1

Boron (B) is an essential micronutrient for plants. Excess B is toxic, but B homeostasis is important for plants (Shorrocks 1997). B is effectively taken up by plants through two distinct B transporters: BOR1 and nodulin-26-like major intrinsic protein (NIP5;1). BOR1 and NIP5;1 are an efflux-type and an influx-

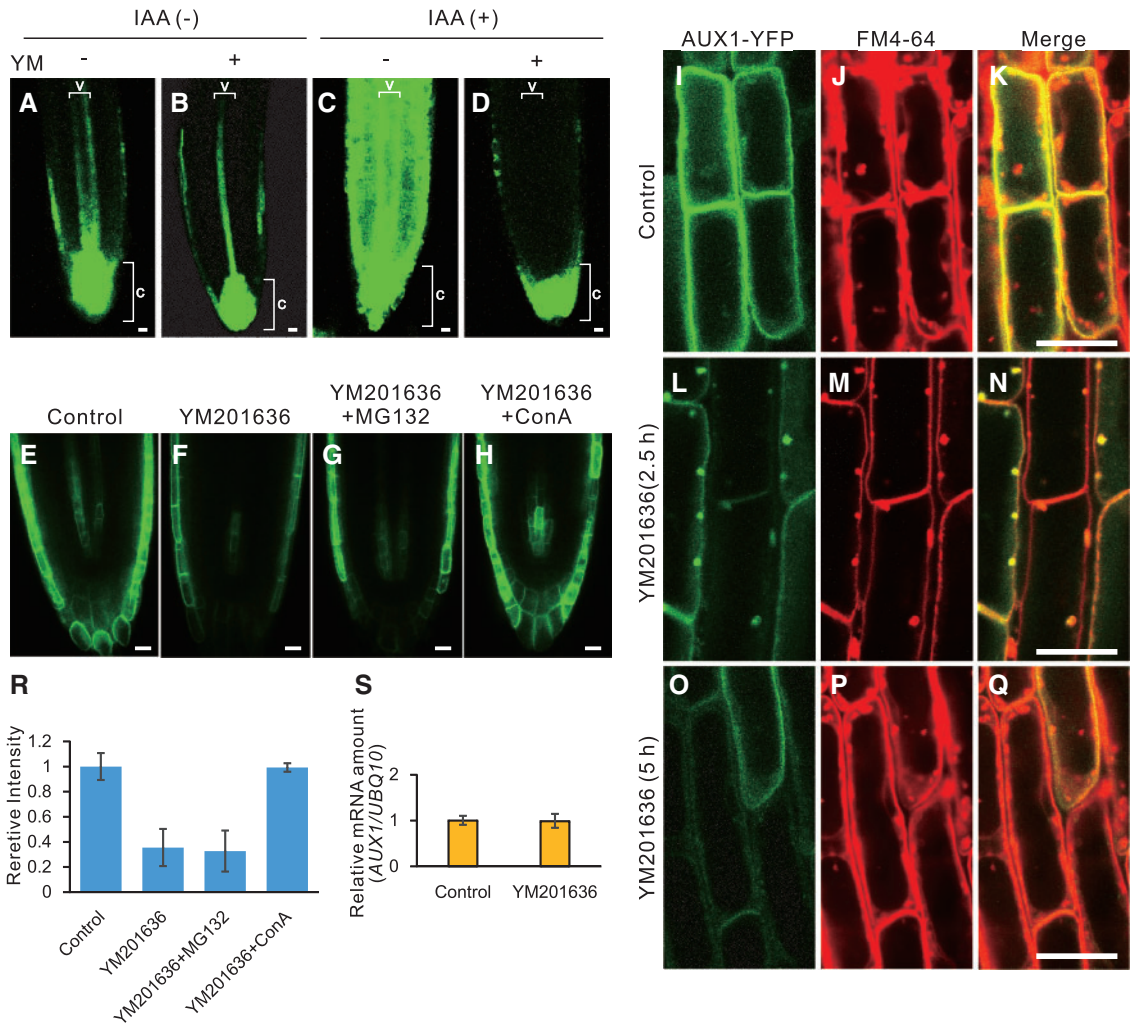

Fig. 2 Inhibition of FAB1 activity reduces the uptake of a non-penetrating auxin and alters the localization pattern of AUX1 in root epidermal cells. The *DR5rev:GFP* transgenic line was grown on the medium in the presence (B, D) or absence (A, C) of YM201636 for 5 d, and then was incubated with (C, D) or without (A, B) 1 μM IAA for 6 h. The fluorescence of GFP was examined using confocal laser scanning microscopy. The letters v and c in the images denote vascular bundle and columella cells, respectively. Five-day-old seedlings of AUX1–YFP-expressing plants were treated with 0.01% DMSO (E, F), 50 μM MG132 for 5 h (G) or 2 μM concanamycin A for 1 h (H), and then the samples were incubated with 1 μM YM201636 for 5 h (F–H). For the FM4-64 labeling experiment, 5-day-old seedlings expressing AUX1–YFP were labeled with 2 μM FM4-64 for 5 min in the presence (L–Q) or absence (I–K) of 1 μM YM201636, and then were examined after 2.5 h (I–N) or 5 h (O–Q) by confocal laser scanning microscopy. The scale bar = 10 μm. (R) The fluorescence intensity of the root tip region of the AUX1–YFP line ($n > 12$) was measured by means of the ImageStudio software. (S) Expression of AUX1 mRNA without or with YM201636 was measured by real-time RT–PCR. The bars represent the mean ± SD ($n = 8$).

type B transporter, respectively, and are polarly localized to the inner and outer plasma membrane domain of root epidermal cells, respectively (Takano et al. 2002, Takano et al. 2006). A high extracellular B concentration causes internalization of BOR1 and subsequently promotes its degradation in the vacuole (Kasai et al. 2011). To examine the effect of YM201636 on the sensitivity to low (0.3 μM), medium (30 μM) and high (300 μM) borate concentrations, 5-day-old WT seedlings—grown on a medium containing 0.3, 30 or 300 μM borate—were transferred to medium containing 0.3, 30 or 300 μM borate with or without YM201636, after which the seedlings were grown for an additional 6 d, and the root and root hair lengths were measured. As shown in **Fig. 3A and B**, the root and root hair lengths of the seedlings grown on the medium containing 0.3 μM B without YM201636 were smaller than those of the seedlings grown on the medium containing 30 μM B. This finding indicates that the growth of seedlings was retarded by the B deficiency, whereas the growth defect was partially reversed by addition of 1 μM YM201636 to the medium. In contrast, the growth of root and root hairs was inhibited when the seedlings were cultivated on the 30 μM borate-containing medium with 1 μM YM201636, as compared with the control condition (no YM201636). In the 300 μM borate-containing medium, the growth of the root and root hair length were equally inhibited regardless of the presence of YM201636.

It was reported that the amount of BOR1 in the presence of 30 μM B (medium B concentration) is decreased via vacuole-mediated degradation as compared with seedlings

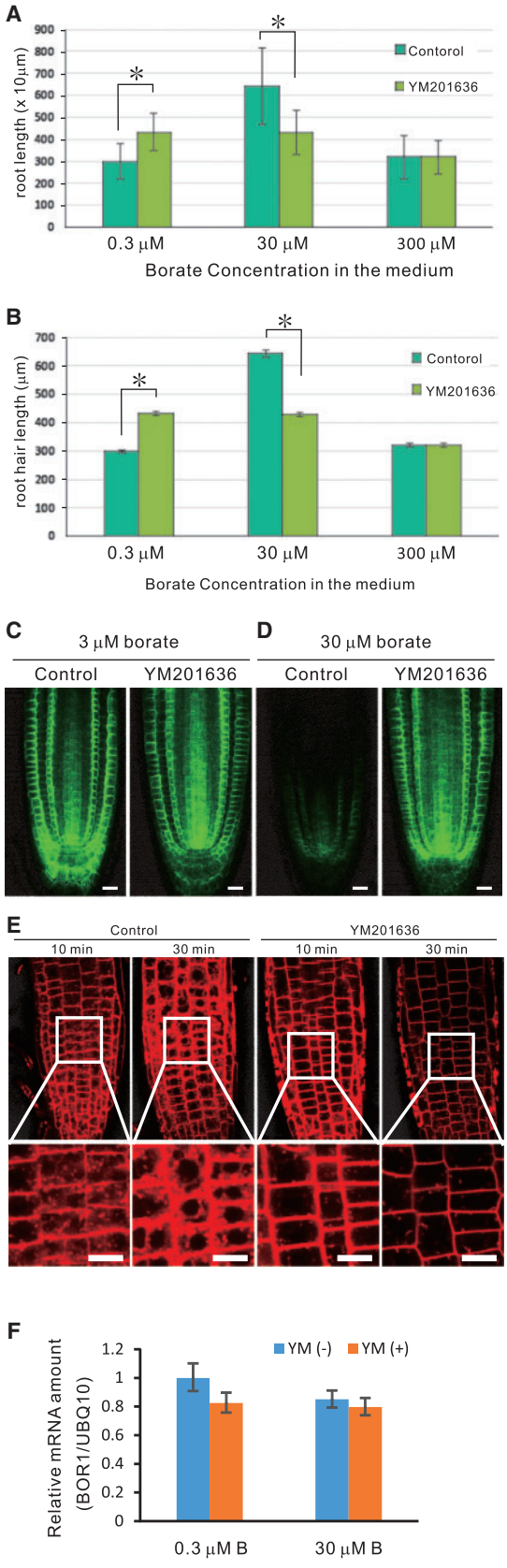

Fig. 3 Sensitivity to a high concentration of borate is decreased by the inhibition of PI(3,5)P_2 synthesis. Five-day-old seedlings of WT grown on a 0.3–3.0 μM borate medium (Takano et al. 2005). At 3 μM borate, the fluorescence of BOR1 on the plasma membrane was unaltered in the presence or absence of YM201636 (**Fig. 3C**). Nevertheless, the amount of BOR1 on the plasma membrane was not changed at 30 μM borate when the seedlings were treated with 1 μM YM201636, although it decreased without YM201636 because BOR1 was degraded at the same borate concentration (**Fig. 3D**). In the presence of YM201636, endocytosis of a fluorescent endocytosis tracer, FM4-64, was strongly delayed, and this tracer never reached the central vacuolar membrane (**Fig. 3E**). In this condition, the mRNA expression of *BOR1* in the presence of YM201636 was unchanged regardless of the presence of YM201636 (**Fig. 3F**). Thus, we concluded that PI(3,5)P_2 regulates B-dependent BOR1 endocytosis and subsequent degradation in the vacuole through a FAB1-mediated endocytic pathway but not at the transcriptional level.

YM201636 inhibits protein secretion

Protein secretion plays pivotal roles in the assembly and modification of the plant cell wall and in various stress responses (Surpin and Raikhel 2004). In plants, the conventional secretion route to the plasma membrane is believed to go through the Golgi–TGN. In Arabidopsis, an alternative secretion pathway via multivesicular bodies/late endosomes was recently reported (Ebine et al. 2011). To test whether PI(3,5)P_2 is involved in the protein secretion routes, localization of a fluorescent secretion marker, secGFP—which contains an N-terminal signal peptide and is secreted to the apoplast through the default secretory pathway (Batako et al. 2000, Zheng et al. 2004)—was used to determine whether the secretion process is affected by YM201636. In the absence of YM201636, weak secGFP fluorescence was observed only in the apoplastic space, indicating that secGFP is secreted from the cells normally (**Fig. 4A, C**). In the presence of YM201636, however, strong fluorescence of

Fig. 3 Continued
Arabidopsis grown on MGRL medium containing 0.3, 30 or 300 μM borate were transferred to the same MGRL medium in the presence or absence (Control) of 1 μM YM201636, and the root length (A) and the length of root hairs (B) were measured after 6 d. The data are presented as the mean ± SD of 20 seedlings (root length) or the 10 longest root hairs from 20 primary roots. Significant differences between seedlings incubated with or without YM201636 are indicated by an asterisk (Student's *t*-test, $P < 0.001$). Five-day-old seedlings of a BOR1–GFP-expressing plant grown on MGRL medium containing 3 or 30 μM borate were examined by confocal laser scanning microscopy with or without YM201636 treatment. Scale bars = 10 μm. (C and D). Endocytosis of FM4-64 was inhibited by incubation with YM201636. For the FM4-64 labeling experiment, 5-day-old seedlings of WT Arabidopsis were labeled with 2 μM FM4-64 for 5 min in the presence or absence of 1 μM YM201636; later, the plants were examined after 10 or 30 min by confocal laser scanning microscopy. Scale bars = 10 μm (E). Transcripts of *BOR1* in WT seedlings grown on MGRL medium at different borate concentrations (0.3 and 30 μM) in the presence or absence of 1 μM YM201636 in the medium were analyzed by qRT-PCR. Bars represent the mean ± SD ($n = 8$) (F).

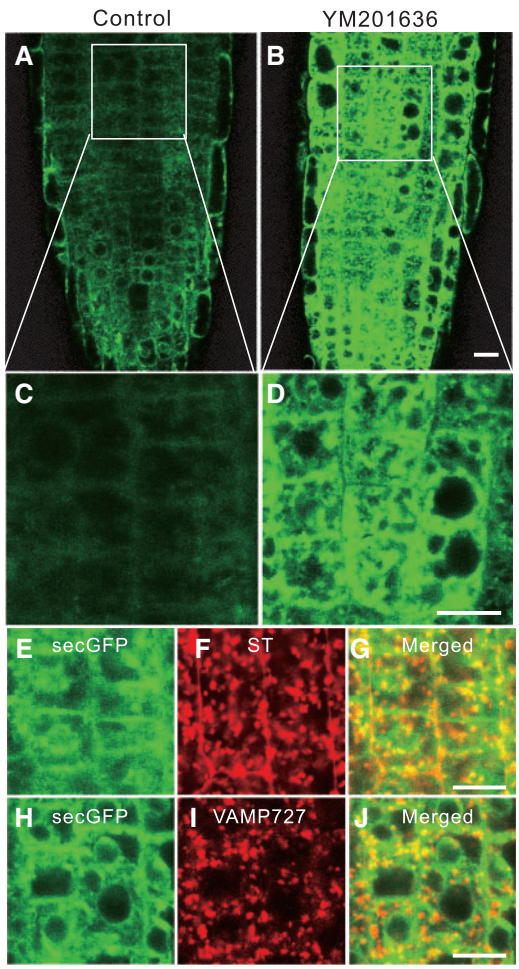

Fig. 4 Secretion of secGFP was inhibited by YM201636. Five-day-old seedlings of secGFP-expressing plants grown on 1/2 MS medium with YM201636 (B and D) or without YM201636 (A and C) were examined by confocal laser scanning microscopy. The root epidermal cells of the transgenic plants co-expressing secGFP (E, G) and ST–mRFP (F, G), or secGFP (H, J) and mRFP–VAMP727 (I, J) were examined under a confocal laser scanning microscope. Scale bars = 10 μm.

secGFP was observed in the cytosol in the form of complex membranous structures but was not observed in the apoplast (**Fig. 4B, D**). The internal membranous structures included tubular ER-like and punctate-endosome-like structures (**Fig. 4B, D**). The punctate structures were overlapping with the staining pattern of a Golgi marker, sialyltransferase (ST)–monomeric red fluorescent protein (mRF)P (**Fig. 4E–G**) and a late-endosome marker, mRFP–VAMP727 (**Fig. 4H–J**), suggesting that secGFP is accumulated in various single-membrane organelles in the secretory pathway. Similarly, conditional knockdown of FAB1A/B caused secretion defect of secGFP (**Supplementary Fig. S4**). Therefore, we concluded that the default secretory pathway is severely impaired by inhibition of PI(3,5)P_2 production.

YM201636 alters the morphological characteristics of late endosomes and vacuoles

In yeast, *fab1* mutants show an enlarged vacuole phenotype (Gary et al. 1998, Morishita et al. 2002). Similarly, in mammalian

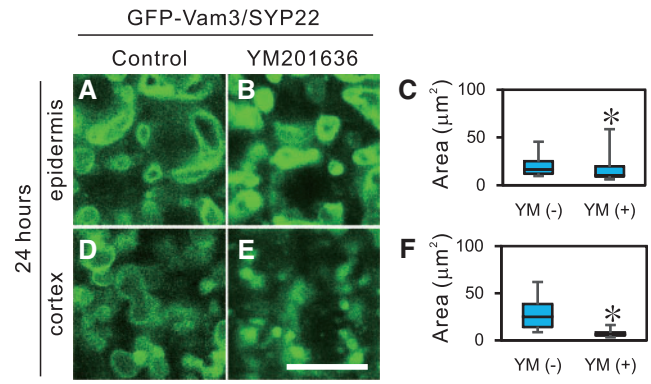

Fig. 5 YM201636 induces morphological changes in the central vacuole. Transgenic plants expressing GFP–VAM3 were grown on 1/2 MS medium for 5 d and then were incubated with (B and E) or without 1 μM YM201636 (A and D) for 24 h. The epidermal cells and cortical cells of the root division zone were examined by confocal laser scanning microscopy. Scale bars = 10 μm. The sizes of the three largest vacuoles in the root division zone were measured by means of ImageJ software, and the size of a single vacuole is presented as the box-and-whisker plots and was analyzed by the Mann–Whitney U-test (*$P < 0.01$; C and F).

cells that overexpress a dominant kinase-inactive mutant of PIKfyve, enlarged lysosomes are also observed (Ikonomov et al. 2001). Thus, a defect in PI(3,5)P_2 production causes defects in the morphology of vacuolar/lysosomal compartments. To study the relationship between PI(3,5)P_2 content and the vacuole morphology in Arabidopsis, the fluorescence patterns of a GFP-tagged vacuolar membrane marker, Arabidopsis vacuolar morphology 3 (AtVAM3)/syntaxin of plants 22 (SYP22)–GFP were examined in the presence and absence of YM201636. The vacuolar membrane structures clearly shrank and formed compact entities in the presence of YM201636 in epidermal cells (**Fig. 5A–C**) and cortical cells (**Fig. 5D–F**) of the root division zone. On the other hand, FAB1A–GFP-labeled late endosomes/multivesicular bodies mostly formed rounded structures in the presence of YM201636 (**Fig. 6A–C**), while the punctate fluorescence pattern of late-endosome/multivesicular body-localized GFP–FYVE1 was completely dispersed throughout the cytosol (**Fig. 6D–F**). Taken together, these data indicate that PI(3,5)P_2 is important for the maintenance of not only late-endosomal structures but also central vacuole structures in Arabidopsis.

Discussion

Membrane dynamics of AUX1 and BOR1 are regulated differently by PI(3,5)P_2

Our previous report revealed that non-penetrating auxin-dependent lateral root formation is severely inhibited by a knockdown or overexpression of *FAB1A/B*, suggesting that the expression and/or localization of an auxin influx transporter, AUX1, can be affected by abnormal *FAB1A/B* expression (Hirano et al. 2011, Hirano and Sato 2011). In the present study, we demonstrated that the uptake of a non-penetrating auxin is

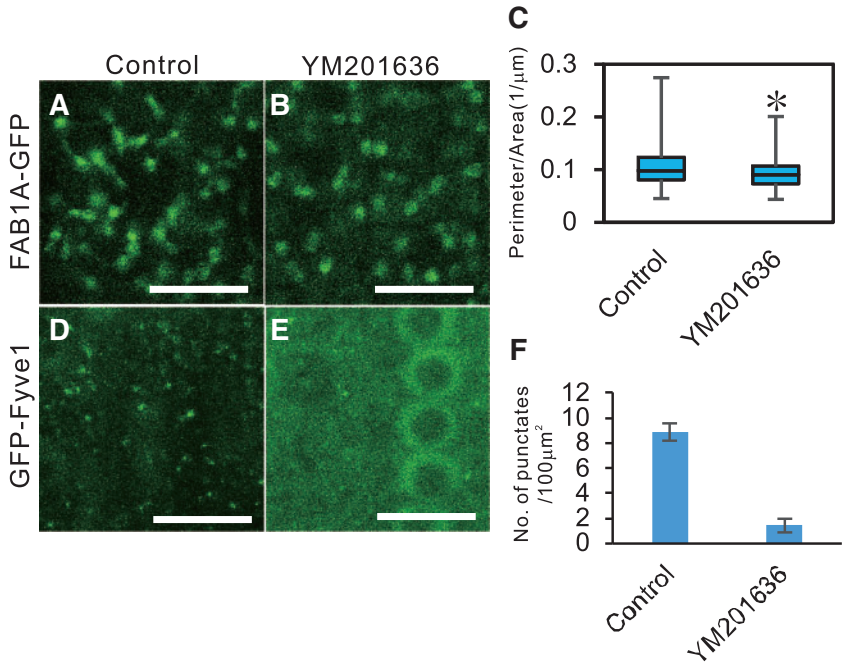

Fig. 6 YM201636 changes the morphological characteristics of vacuoles and late-endosomal protein markers. Five-day-old transgenic plants expressing FAB1–GFP or GFP–FYVE1 were grown on 1/2 MS medium and incubated with (B and E) or without 1 μM YM201636 (A and E) for 2 h; the fluorescence was examined by confocal laser scanning microscopy. Scale bars = 10 μm. The area and perimeter of vacuoles and the number of spots were measured by means of ImageJ software, are presented as box-and-whisker plots and were analyzed by the Mann–Whitney U-test (*$P < 0.01$) (C) or by means of a bar graph. Significant differences between seedlings incubated with or without YM201636 are indicated by an asterisk (Student's *t*-test, $P < 0.001$) (F).

strongly inhibited by YM201636 treatment. In the presence of YM201636, the AUX1–YFP fusion protein is internalized and probably degraded in the vacuole.

On the other hand, BOR1 internalization and subsequent degradation in the vacuole at higher B concentrations (Takano et al. 2010, Kasai et al. 2011, Scheuring et al. 2011) were strongly inhibited by YM201636 treatment at 30 μM borate. In contrast, at 0.3 μM borate, BOR1–GFP fluorescence was not significantly different from that in the control (**Fig. 3C, D**). We previously reported that FAB1 dysfunction delays endocytosis (Hirano et al. 2011). This delayed endocytosis was attributed to the maturation defect in late endosomes/multivesicular bodies caused by the decrease in PI(3,5)P_2 content (Hirano et al. 2015). In this study, we also observed that the endocytosis process is severely impaired by YM201636 treatment (**Fig. 3E**). Given that the effect of YM201636 is the inhibition of the maturation of FAB1-positive endosomes thereby causing delayed endocytosis, the inhibition of BOR1 endocytosis by YM201636 may be mediated by the dysfunction of maturation of FAB1-positive endosomes, so that BOR1 can no longer be internalized and transported to the vacuole via the FAB1-positive late endosomes/multivesicular bodies.

AUX1, also a plasma membrane protein, behaved differently at low PI(3,5)P_2 concentrations. Namely, YM201636 blocked the internalization of BOR1, while AUX1 was endocytosed and degraded. How can the differences in subcellular dynamics of these two proteins at low PI(3,5)P_2 concentrations be explained? It is reported that AUX1 follows a trafficking pathway different from that of other polarized membrane proteins. For example, AUX1 dynamics show different sensitivity to inhibitors of trafficking and are independent of the endosomal trafficking regulator ARF-GEF, known as GNOM in Arabidopsis (Kleine-Vehn et al. 2006, Geldner et al. 2003). PIN2, but not AUX1 or PIN1, is transported through AtSNX1-containing endosomes, and AUX1 trafficking is not affected in either a *snx1* or a *vps29* mutant (Jaillais et al. 2006, Jaillais et al. 2007). Thus, there are multiple endocytosis and recycling pathways for plasma membrane proteins in Arabidopsis. Most probably, FAB1/PI(3,5)P_2 is involved in the regulation of multiple endocytic pathways via distinct mechanisms.

The secretory pathway is affected by YM201636 treatment

Although newly synthesized secretory proteins are known to be transported from the ER through the Golgi apparatus to the TGN en route to the plasma membrane or to the extracellular medium (Richter et al. 2009), it is unknown whether the secretory pathway passes through late endosomes/multivesicular bodies. We found that the process of secretion of secGFP is inhibited by YM201636 (**Fig. 4**), suggesting that PI(3,5)P_2-mediated membrane trafficking is involved in the default secretory process in Arabidopsis.

In plants, secretory traffic from the TGN to the plasma membrane is regulated by RABA4b and phosphatidylinositol-4 kinase β-1 (PI4Kβ-1). RABA4b and PI4Kβ-1 are co-localized to budding secretory vesicles in the TGN, and the *pi4kb1pi4kb2* double mutant has aberrant sizes of secretory vesicles (Kang

et al. 2011). Furthermore, PI4P 5-kinases, PIP5K1 and PIP5K2, and their product, PI(4,5)P_2, are specifically enriched in the apical and basal polar plasma membrane domains, and PI(4,5)P_2 influences polarization of PINs (auxin transporters) (Ischebeck et al. 2013, Tejos et al. 2014). We found that the secretion marker secGFP is down-regulated by YM201636 (**Fig. 5**), suggesting that PI(3,5)P_2 also controls the secretory traffic. We previously reported that the loss of FAB1 function and inhibition of PI(3,5)P_2 production cause a release of late-endosomal effector proteins, thereby impairing the early stage of late-endosome maturation (Hirano et al. 2015). Accordingly, the secretion defect caused by the inhibition of PI(3,5)P_2 synthesis may result from the defect in the late-endosome maturation; therefore, the secretory route possibly passes through late endosomes in Arabidopsis.

The defects in the vacuolar transport pathway and vacuolar structure

In yeast, FAB1 and PI(3,5)P_2 regulate endosomal trafficking to the vacuole/lysosomes. PI(3,5)P_2 is present on the external membrane of multivesicular bodies (Odorizzi et al. 1998). The yeast *fab1* mutant shows enlarged vacuoles, with a defect in vacuolar acidification and osmoregulation. It also has a growth defect at elevated temperatures because of impairment of both the retrograde vesicle transport from vacuoles to the TGN and the anterograde pathway to the vacuole (Gary et al. 1998, Odorizzi et al. 1998). In Arabidopsis, the *fab1a:fab1b* double mutant shows male gametophyte mortality. Mutant pollen grains have severe defects in vacuolar reorganization (Whitley et al. 2009), while a loss of FAB1 function impairs endomembrane homeostasis, including endocytosis, vacuole formation and vacuolar acidification (Hirano et al. 2011). Here, we found that YM202636 treatment diminished luminal vacuoles (**Fig. 5**) but caused circulation of FAB1-positive late endosomes/multivesicular bodies (**Fig. 6A–C**) and induced the release of GFP–FYVE1 from the endosome membrane (**Fig. 6D–F**).

The FAB1, YOTB, VAC1 and EEA1 (FYVE) domain-containing protein—FYVE1/FREE1—has been implicated in intracellular trafficking. FYVE1/FREE1 is localized to late endosomes and interacts with Src homology-3 domain-containing proteins. A T-DNA insertion mutant, *fyve1/free1*, shows abnormal vacuolar morphology where small fragmented vacuoles are interconnected, and is defective in ubiquitin-mediated protein degradation, vacuolar transport and autophagy (Gao et al. 2015, Kolb et al. 2015). Because we observed similar small vacuolar structures caused by the YM201636 treatment (**Fig. 5**), we assumed that the smaller vacuolar structure may be formed by a release of the FYVE1/FREE1 protein from the late-endosomal membrane because of lower PI(3,5)P_2 concentrations.

Similar morphological defects in the vacuole and in late endosomes/multivesicular bodies were also observed in a RABG3f plant Rab7 small GTPase member dominant-negative mutant. Ectopic expression of this mutant induced simultaneous formation of abnormal fragmented vacuoles and enlarged pre-vacuolar compartments (Cui et al. 2014). Enlarged late endosomes/multivesicular bodies were also reported in *sand-1* (Singh et al. 2014) and after wortmannin treatment (Jaillais et al. 2006, Vermeer et al. 2006). Previously, we showed that FAB1, and/or its product PI(3,5)P_2, is involved in the early stages of late endosome/multivesicular body maturation, recruiting late-endosome effector proteins (Hirano et al. 2015). If the maturation of late endosomes/multivesicular bodies is inhibited by a reduction in PI(3,5)P_2 concentration, then SAND-CCZ1-mediated Rab5 (ARA7 in Arabidopsis) to Rab7 (RABG3f in Arabidopsis) conversion may be stopped. Consequently, multiple membrane trafficking routes, including the recycling pathway of BOR1 and the secretion and vacuolar transport pathways, can be impaired. In the case of AUX1, alternative trafficking pathways rather than the late-endosome/multivesicular body-dependent pathway to the vacuole (Ebine et al. 2014) may be affected by a so far unknown PI(3,5)P_2-dependent mechanism (**Fig. 7**). Additional studies are needed to dissect the PI(3,5)P_2-mediated membrane trafficking pathways in plants.

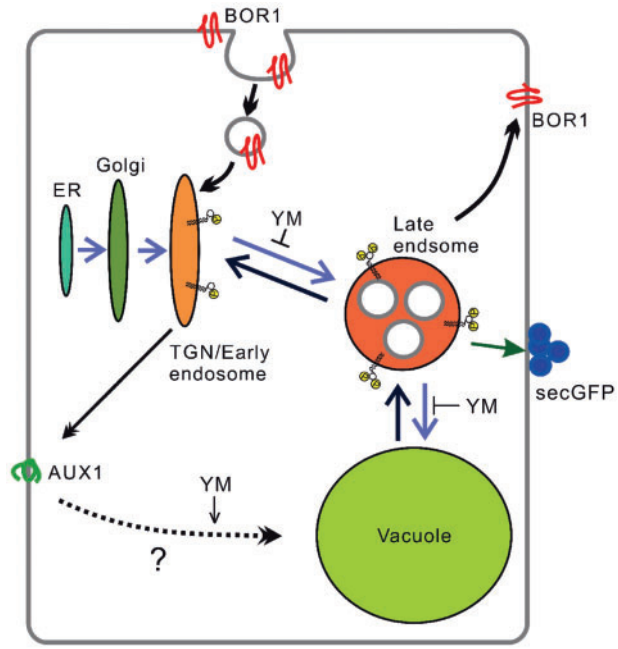

Fig. 7 A schematic model of the membrane trafficking routes regulated by FAB1-positive endosomes in Arabidopsis root cells. BOR1 protein is recycled via the TGN/early endosomes and FAB1-positive late endosomes (LEs) to the plasma membrane (PM). SecGFP is secreted to the apoplast via the TGN/early endosome and FAB1-positive endosomes. AUX1 is endocytosed and targeted for degradation probably in the vacuole when PI(3,5)P_2 synthesis is inhibited. YM, YM201636.

Materials and Methods

Plant growth conditions

The *A. thaliana* ecotype Col-0 served as the WT in all experiments in this study. The plants were grown under white light in a cycle of 16 h light and 8 h dark at 22°C on half-strength Murashige and Skoog (1/2 MS) medium or

MGRL medium (Fujiwara et al. 1992) containing various borate concentrations.

Confocal laser scanning microscopy

GFP, mRFP and FM4-64 fluorescent signals and differential interference contrast (DIC) images were obtained using a laser scanning microscope (Eclipse E600; Nikon Corp.) equipped with a C1si-ready confocal system (Nikon Corp.) at the following wavelengths for excitation and detection: 488 and 515–530 nm for GFP and 543 and 605–675 nm for mRFP and FM4-64. The acquired images were processed in the vendor's software (EZ-C1; Nikon Corp.).

Quantitative RT-PCR (qRT-PCR)

Total RNA was extracted from the transgenic lines. Then, reverse transcription was performed using ReverTra Ace qPCR RT Master Mix (TOYOBO) for cDNA synthesis from 1 μg of total RNA in the reaction mixture; a 1 μl sample was taken for a subsequent PCR. For qRT-PCR, gene expression was monitored using 1 μl of diluted cDNA in the Thunderbird SYBR qPCR Mix (TOYOBO). qRT-PCR was performed using primer pairs AUX1-F (5′-CGCTCACATGCTCAC TTACC-3′) and AUX1-R (5′-GCATAAAGAACGGTGGCTTC-3′) for AUX1 and BOR1-F (5′-AGAAGCAGAAAAGCCAGATCA-3′) and BOR1-R (5′-TGGTACAC CATGTCAGCTATTAAGC-3′) for BOR1 and UBQ10-F (5′- GGCCTTGTATAAT CCCTGATGAATAAG-3′) and UBQ10-R (5′- AAAGAGATAACAGGAACGGAA ACATAGT-3′) for ubiquitin 10 (UBQ10, At4g05320), which served as an internal standard. Quantification of five independent samples was performed for each data point.

Measurement of root length

Roots were examined in 5-day-old seedlings grown on 1/2 MS agar plates supplemented with 1 μM YM201636, 1 μM 17-β-estradiol or 0.01% DMSO (control). Their lengths were measured using ImageJ software (National Institutes of Health, USA).

YM201636 treatment and phosphoinositide analysis

Polyphosphoinositide levels were measured according to the method of Munnik and Zarza (2013). Briefly, radioactive PIP_2 levels were measured by labeling 5-day-old seedlings (three per tube in triplicate) of WT and *FAB1A*-overexpressing lines with 0.37 MBq of carrier-free [^{32}P]orthophosphate overnight (~16 h). The next day, seedlings were incubated with or without 1 μM YM201636 for 2 h, after which lipids were extracted, separated by TLC (Meijer et al. 1999) and quantified by means of Image Studio software (LI-COR).

Supplementary data

Supplementary data are available at PCP online.

Funding

This work was supported by the Ministry of Education, Culture, Sports, Science and Technology of Japan [a grant-in-aid for Scientific Research (B) (16H05068 to M.H.S.), a grant on Innovative Areas (25119720 to M.H.S.)]; and Kyoto Prefectural University [Strategic Research Funds (to M.H.S.)].

Acknowledgments

We thank J. Friml (Institute of Science and Technology, Austria) for providing *DR5rev:GFP* and AUX1-YFP lines, J. Takano (Hokkaido University) for the BOR-GFP line, and E. Isono (Max Planck Institute for Developmental Biology) for the FYVE1-GFP line. We also thank K. Tamura and I.-H. Nishimura (Kyoto University) for confocal microscopic analyses and fruitful discussions.

Disclosures

The authors have no conflicts of interest to declare.

References

Bak, G., Lee, E.J., Lee, Y., Kato, M., Segami, S., Sze, H., et al. (2013) Rapid structural changes and acidification of guard cell vacuoles during stomatal closure require phosphatidylinositol 3,5-bisphosphate. *Plant Cell* 25: 2202–2216.

Balla, T. (2013) Phosphoinositides: tiny lipids with giant impact on cell regulation. *Physiol. Rev.* 93: 1019–1137.

Batoko, H., Zheng, H.Q., Hawes, C. and Moore, I. (2000) A rab1 GTPase is required for transport between the endoplasmic reticulum and golgi apparatus and for normal Golgi movement in plants. *Plant Cell* 12: 2201–2218.

Bonifacino, J.S. and Glick, B.S. (2004) The mechanisims of vesicle budding and fusion. *Cell* 116: 153–166.

Cui, Y., Zhao, Q., Gao, C., Ding, Y., Zeng, Y., Ueda, T., et al. (2014) Activation of the Rab7 GTPase by the MON1–CCZ1 complex is essential for PVC-to-vacuole trafficking and plant growth in Arabidopsis. *Plant Cell* 26: 2080–2097.

Dettmer, J., Hong-Hermesdorf, A., Stierhof, Y.-D. and Schumacher, K. (2006) Vacuolar H^+-ATPase activity is required for endocytic and secretory traffcking in Arabidopsis. *Plant Cell* 18: 715–730.

Drakakaki, G. and Dandekar, A. (2013) Protein secretion: how many secretory routes does a plant cell have? *Plant Sci.* 203–204: 74–78.

Ebine, K., Fujimoto, M., Okatani, Y., Nishiyama, T., Goh, T., Ito, E., et al. (2011) A membrane trafficking pathway regulated by the plant-specific RAB GTPase ARA6. *Nat. Cell Biol.* 13: 853–859.

Ebine, K., Inoue, T., Ito, J., Ito, E., Uemura, T., Goh, T., et al. (2014) Plant vacuolar trafficking occurs through distinctly regulated pathways. *Curr. Biol.* 24: 1375–1382.

Fujiwara, T., Hirai-Yokota, M., Chino, M., Komeda, Y. and Naito, S. (1992) Effects of sulfur nutrition on expression of the soybean storage protein genes in transgenic petunia. *Plant Physiol.* 99: 263–268.

Gao, C., Zhuang, X., Cui, Y., Fu, X., He, Y., Zhao, Q., et al. (2015) Dual roles of an Arabidopsis ESCRT component FREE1 in regulating vacuolar protein transport and autophagic degradation. *Proc. Natl Acad. Sci. USA* 112: 1886–1891.

Gary, J.D., Wurmser, A.E., Bonangelino, C.J., Weisman, L.S. and Emr, S.D. (1998) Fab1p is essential for PtdIns(3)P 5-kinase activity and the maintenance of vacuolar size and membrane homeostasis. *J. Cell Biol.* 143: 65–79.

Geldner, N., Anders, N., Wolters, H., Keicher, J., Kornberger, W., Muller, P., et al. (2003) The Arabidopsis GNOM ARF-GEF mediates endosomal recycling, auxin transport, and auxin-dependent plant growth. *Cell* 112: 219–230.

Heilmann, M. and Heilmann, I. (2015) Plant phosphoinositides—complex networks controlling growth and adaptation. *Biochim. Biophys. Acta* 1851: 759–769.

Hirano, T., Matsuzawa, T., Takegawa, K. and Sato, M.H. (2011) Loss-of-function and gain-of-function mutations in FAB1A/B impair endomembrane homeostasis, conferring pleiotropic developmental abnormalities in Arabidopsis. *Plant Physiol.* 155: 797–807.

Hirano, T., Munnik, T. and Sato, M.H. (2015) Phosphatidylinositol 3-phosphate 5-kinase, FAB1/PIKfyve mediates endosome maturation to establish endosome–cortical microtubule interaction in Arabidopsis. *Plant Physiol.* 169: 1961–1974.

Ikonomov, O.C., Sbrissa, D. and Shisheva, A. (2001) Mammalian cell morphology and endocytic membrane homeostasis require enzymatically active phosphoinositide 5-kinase PIKfyve. *J. Biol. Chem.* 276: 26141–26147.

Ischebeck, T., Werner, S., Krishnamoorthy, P., Lerche, J., Meijon, M., Stenzel, I., et al. (2013) Phosphatidylinositol 4,5-bisphosphate jnfluences PIN polarization by controlling clathrin-mediated membrane trafficking in Arabidopsis. *Plant Cell* 25: 4894–4911.

Jaillais, Y., Fobis-loisy, I., Miege, C., Rollin, C. and Gaude, T. (2006) AtSNX1 defines an endosome for auxin-carrier trafficking in Arabidopsis. *Nature* 443: 106–109.

Jaillais, Y., Santambrogio, M., Rozier, F., Fobis-Loisy, I., Miège, C. and Gaude, T. (2007) The retromer protein VPS29 links cell polarity and organ initiation in plants. *Cell* 130: 1057–1070.

Jahn, R., Lang, T. and Südhof, T.C. (2003) Membrane fusion. *Cell* 112: 519–533.

Jean, S. and Kiger, A.A. (2012) Coordination between RAB GTPase and phosphoinositide regulation and functions. *Nat. Rev. Mol. Cell Biol.* 13: 463–470.

Jefferies, H.B.J., Cooke, F.T., Jat, P., Boucheron, C., Koizumi, T., Hayakawa, et al. (2008). A selective PIKfyve inhibitor blocks PtdIns(3,5)P(2) production and disrupts endomembrane transport and retroviral budding. *EMBO Rep.* 13: 164–170.

Kang, B.-H., Nielsen, E., Preuss, M.L., Mastronarde, D. and Staehelin, L.A. (2011) Electron tomography of RabA4b- and PI-4Kβ1-labeled trans Golgi network compartments in Arabidopsis. *Traffic* 12: 313–329.

Kasai, K., Takano, J., Miwa, K., Toyoda, A. and Fujiwara, T. (2011) High boron-induced ubiquitination regulates vacuolar sorting of the BOR1 borate transporter in *Arabidopsis thaliana*. *J. Biol. Chem.* 286: 6175–6183.

Kleine-Vehn, J., Dhonukshe, P., Swarup, R., Bennett, M. and Friml, J. (2006) Subcellular trafficking of the Arabidopsis auxin influx carrier AUX1 uses a novel pathway distinct from PIN1. *Plant Cell* 18: 3171–3181.

Kolb, C., Nagel, M.-K., Kalinowska, K., Hagmann, J., Ichikawa, M., et al. (2015) FYVE1 is essential for vacuole biogenesis and intracellular trafficking in Arabidopsis. *Plant Physiol.* 167: 1361–1373.

Krishnamoorthy, P., Sanchez-Rodriguez, C., Heilmann, I. and Persson, S. (2014) Regulatory roles of phosphoinositides in membrane trafficking and their potential impact on cell-wall synthesis and re-modelling. *Ann. Bot.* 114: 1049–1057.

McCartney, A.J., Zhang, Y. and Weisman, L.S. (2014) Phosphatidylinositol 3,5-bisphosphate: low abundance, high significance. *Bioessays* 36: 52–64.

Morishita, M., Morimoto, F., Kitamura, K., Koga, T., Fukui, Y., Maekawa, et al. (2002) Phosphatidylinositol 3-phosphate 5-kinase is required for the cellular response to nutritional starvation and mating pheromone signals in *Schizosaccharomyces pombe*. *Genes Cells* 7: 199–215.

Munnik, T. and Zarza, X. (2013) Analyzing plant signaling phospholipids through 32Pi-labeling and TLC. *Methods Mol. Biol.* 1009: 3–15.

Odorizzi, G., Babst, M. and Emr, S.D. (1998) Fab1p PtdIns(3)P 5-kinase function essential for protein sorting in the multivesicular body. *Cell* 95: 847–858.

Park, M. and Jürgens, G. (2011) Membrane traffic and fusion at post-Golgi compartments. *Front. Plant Sci.* 2: 111.

Richter, S., Voss, U., Jürgens, G. (2009) Post-Golgi traffic in plants. *Traffic* 10: 819–828.

Scheuring, D., Viotti, C., Krüger, F., Künzl, F., Sturm, S., Bubeck, J., et al. (2011) Multivesicular bodies mature from the trans-Golgi network/early endosome in Arabidopsis. *Plant Cell* 23: 3463–3481.

Shorrocks, V.M. (1997) The occurrence and correction of boron deficiency. *Plant Soil* 193: 121–148.

Simon, M.L.A., Platre, M.P., Assil, S., Van Wijk, R., Chen, W.Y., Chory, J., et al. (2014) A multi-colour/multi-affinity marker set to visualize phosphoinositide dynamics in Arabidopsis. *Plant J.* 77: 322–337.

Singh, M.K., Krüger, F., Beckmann, H., Brumm, S., Vermeer, J.E.M., Munnik, T., et al. (2014) Protein delivery to vacuole requires SAND protein-dependent Rab GTPase conversion for MVB-vacuole fusion. *Curr. Biol.* 24: 1383–1389.

Staehelin, L.A. and Chapman, R.L. (1987) Secretion and membrane recycling in plant cells: novel intermediary structures, visualized in ultra-rapidly frozen sycamore and carrot suspension-culture cells. *Planta* 171: 43–57.

Surpin, M. and Raikhel, N. (2004) Traffic jams affect plant development and signal transduction. *Nat. Rev. Mol. Cell Biol.* 5: 100–109.

Takano, J., Miwa, K., Yuan, L., von Wirén, N. and Fujiwara, T. (2005) Endocytosis and degradation of BOR1, a boron transporter of Arabidopsis thaliana, regulated by boron availability. *Proc. Natl Acad. Sci. USA* 102: 12276–12281.

Takano, J., Noguchi, K., Yasumori, M., Kobayashi, M., Gajdos, Z., Miwa, K., et al. (2002) Arabidopsis boron transporter for xylem loading. *Nature* 420: 337–340.

Takano, J., Tanaka, M., Toyoda, A., Miwa, K., Kasai, K., Fuji, K., et al. (2010) Polar localization and degradation of Arabidopsis boron transporters through distinct trafficking pathways. *Proc. Natl Acad. Sci. USA* 107: 5220–5225.

Takano, J., Wada, M., Ludewig, U., Schaaf, G., Von Wirén, N. and Fujiwara, T. (2006) The Arabidopsis major intrinsic protein NIP5;1 is essential for efficient boron uptake and plant development under boron limitation. *Plant Cell* 18: 1498–1509.

Tejos, R., Sauer, M., Vanneste, S., Palacios-Gomez, M., Li, H., Heilmann, M., et al. (2014) Bipolar plasma membrane distribution of phosphoinositides and their requirement for auxin-mediated cell polarity and patterning in Arabidopsis. *Plant Cell* 26: 2114–2128.

Toyooka, K., Goto, Y., Asatsuma, S., Koizumi, M., Mitsui, T. and Matsuoka, K. (2009) A mobile secretory vesicle cluster involved in mass transport from the Golgi to the plant cell exterior. *Plant Cell* 21: 1212–1229.

Uemura, T., Ueda, T., Ohniwa, R.L., Nakano, A., Takeyasu, K. and Sato, M.H. (2004) Systematic analysis of SNARE molecules in Arabidopsis: dissection of the post-Golgi network in plant cells. *Cell Struct. Funct.* 29: 49–65.

Vermeer, J.E.M., van Leeuwen, W., Tobeña-Santamaria, R., Laxalt, A.M., Jones, D.R., Divecha, N., et al. (2006) Visualization of PtdIns3 *P* dynamics in living plant cells. *Plant J.* 47: 687–700.

Whitley, P., Hinz, S. and Doughty, J. (2009) Arabidopsis FAB1/PIKfyve proteins are essential for development of viable pollen. *Plant Physiol.* 151: 1812–1822.

Winter, D., Vinegar, B., Nahal, H., Ammar, R., Wilson, G.V. and Provart, N.J. (2007) An 'Electronic Fluorescent Pictograph' browser for exploring and analyzing large-scale biological data sets. *PLoS One* 2: e718.

Zheng, H., Kunst, L., Hawes, C. and Moore, I. (2004) A GFP-based assay reveals a role for RHD3 in transport between the endoplasmic reticulum and Golgi apparatus. *Plant J.* 37: 398–414.